Developmental Biology **251,** 241–257 (2002)
doi:10.1006/dbio.2002.0812

The Regulation and Action of Myostatin as a Negative Regulator of Muscle Development during Avian Embryogenesis

Helge Amthor,*,†,[1] Ruijin Huang,†,[1] Iain McKinnell,* Bodo Christ,† Ravi Kambadur,‡ Mridula Sharma,‡ and Ketan Patel*,[2]

**Department of Veterinary Basic Sciences, Royal Veterinary College, Royal College Street, London NW1 OTU, England; †Institute of Anatomy, University of Freiburg, P. O. Box 111, D-79001, Freiburg, Germany; and ‡Animal Genomics, AgResearch, Private Bag 3123, East St., Hamilton 2001, New Zealand*

Myostatin is a potent inhibitor of muscle growth. Genetic deletion of *Myostatin* leads to massive hyperplasia and hypertrophy of skeletal muscle. However, the overall muscle pattern is preserved. We show that, during chick embryonic development, *Myostatin* is expressed at stages and positions unlikely to influence qualitative muscle development. In the somites, *Myostatin* is predominantly expressed in a central domain of the dermomyotome but not at the dorsomedial and ventrolateral lips, where most cells for myotomal elongation are recruited. During limb bud development, *Myostatin* is transiently expressed at early stages in both myogenic and nonmyogenic regions. *Myostatin* is reexpressed during limb bud development at a time when splitting of muscle is underway. Heterotopically developed wing buds that fail to form muscle still express *Myostatin*. This demonstrates that, in the limb, not all *Myostatin*-expressing cells are of myogenic origin. Ectoderm and Sonic hedgehog have different effects on the expression of *Myostatin* dependent on stages at which the operation was performed and the length of the postoperative period. Finally, we show that application of Myostatin protein into the developing limb bud results in a down-regulation of *Pax-3* and *Myf-5*, both genes associated with proliferation of myogenic cells; and, furthermore, Myostatin also prevents the expression of *MyoD*, a gene associated with muscle differentiation. The long-term effect of Myostatin treatment leads to a deficiency of limb muscle. Therefore, Myostatin negatively affects gene expression of transcription factors, which are necessary for establishing myogenic cell identity.

Key Words: **chick; embryo; muscle; myogenesis; myostatin; development; dermis; somites; Pax-3; MyoD; Myf-5.**

INTRODUCTION

Regulation of body size is one of the most fascinating aspects of developmental biology, as animals even within a species can display tremendous differences in proportion without changing the basic body plan. The development of the muscle mass has been of intensive research interest because it can significantly vary in its bulk without changing the structure of the whole body (Christ *et al.*, 2001). Numerous studies suggest that the development of muscle is regulated by secreted factors originating from both myogenic and nonmyogenic sources.

We have previously presented data which suggest that bone morphogenetic proteins (BMPs), members of the TGF-β superfamily of secreted proteins, and their antagonists Follistatin and Noggin may influence embryonic muscle growth (Amthor *et al.*, 1999, 2002). During embryonic development, factors such as BMPs have been implicated not only in regulating the growth but also in the final positioning of muscle (Amthor *et al.*, 1998).

However, the influence of TGF-β family members on muscle development has been most dramatically demonstrated following the genetic deletion of *Myostatin* (also known as *GDF-8*). *Myostatin*-null mice display a dramatic widespread phenotype, with muscle of mutant animals

[1] These authors contributed equally to this work.

[2] To whom correspondence should be addressed. Fax: +0207-388-1027. E-mail: kpatel@rvc.ac.uk.

0012-1606/02 $35.00

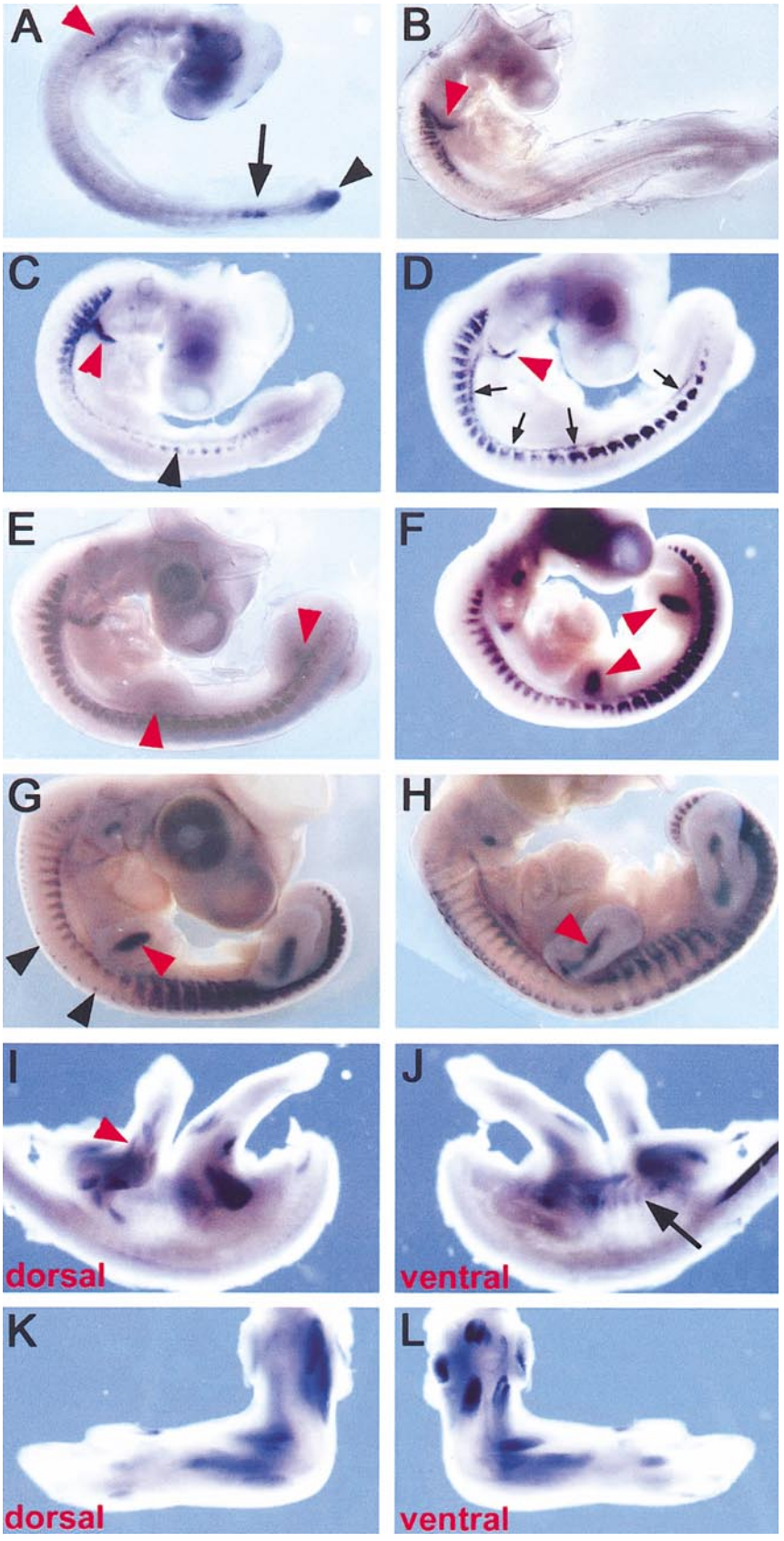

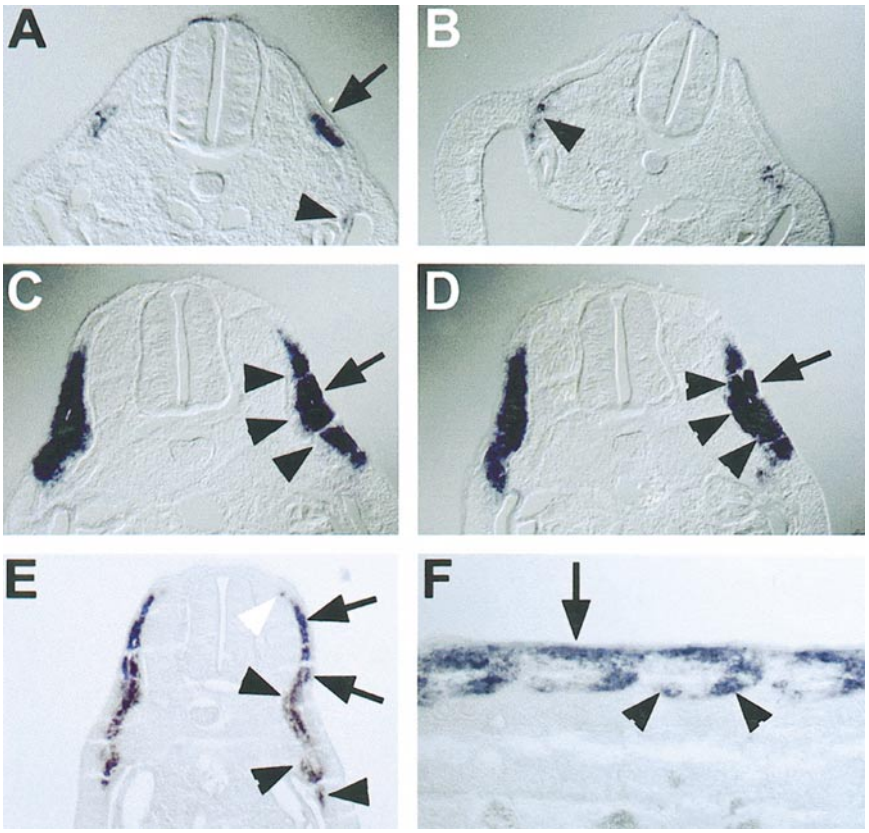

FIG. 2. Tissue expression of *Myostatin* during somite development. (A, B) *Myostatin* expression in the central domain of the dermomyotome at interlimb level at HH stage 20 (A, arrow) and in cells ventral to the dermomyotome (A, B, arrowheads). (C) Transverse section through the centre of a somite at interlimb level of an HH stage 22 embryo shows *Myostatin* expression in the dermomyotome (arrow) but no expression in the dorsomedial and ventrolateral dermomyotomal lips. Note that there is no expression in the myotome (arrowheads). (D) Transverse section through the cranial part of a somite at interlimb level of same embryo as shown in (C) (HH stage 22). At this somite level, the myotome does express *Myostatin* (arrowheads) additionally to the dermomyotomal expression (arrow). (E) *Myostatin* expression in the dermomyotome (arrows) and in the hypaxial part of the myotome (black arrowheads) and in the most dorsally located myotomal tip (white arrowhead) at interlimb level of HH stage 25 somites. (F) *Myostatin* expression in the dermomyotome (arrow) and in the rostral and caudal part of the myotome at interlimb level (arrowheads) after longitudinal sectioning of an HH stage 25 embryo.

FIG. 1. Developmental time course of avian embryonic *Myostatin* expression. (A) *Myostatin* expression in the two most caudally situated somites (black arrow), lateral aspects of occipital somites (red arrowhead), and in the tail bud (black arrowhead) at HH stage 15. (B) *Myostatin* expression in the ventral part of occipital and cervical somites and cells which migrate in the tongue (red arrowhead) at HH stage 17. (C) *Myostatin* expression in the medial part of somites at interlimb level (black arrowhead), in the ventral part of occipital and cervical somites, and in cells which migrate in the tongue (red arrowhead) at HH stage 19. (D) *Myostatin* expression in all somites (except tailbud somites) and prospective tongue muscle (red arrowhead) at HH stage 20. Expression is confined to the central somite part and excluded of the dorsomedial and ventrolateral somite part. Additionally, Myostatin is expressed as a continuous band laterally to somites (black arrows). (E) *Myostatin* expression in somites similar to (D) and first expression in a proximocentral domain of limb buds (red arrowheads) at HH stage 21. (F) Distal extension of centrally located *Myostatin* expression domain in limb buds (red arrowheads) at HH stage 22. At trunk level, *Myostatin* expression extends to the tail bud somites and expression declines in occipital and cervical somites. (G) *Myostatin* expression extends more dorsomedially and ventrolaterally in interlimb somites at HH stage 25 compared with younger stages. Additional up-regulation of *Myostatin* expression at the most dorsomedial part of the somites (black arrowheads). Expression in the wing bud (red arrowhead). (H) High expression in the hypaxial part of the myotomes at interlimb level at HH stage 27. Expression in the wing bud declines (red arrowhead). (I) Dorsal view at an HH stage 29 embryo. Expression is found only in some muscles of the wing bud (red arrowhead). (J) Ventral view of embryo shown in (I). Expression only in hypaxial trunk muscle (black arrow). (K, L) Dorsal view (K) and ventral view (L) of an HH stage 32 wing bud. Expression is found in some but not all wing muscles.

weighing two to three times that of wild-type mice (McPherron and Lee, 1997). Muscle enlargement is due to an increase in the number of muscle fibres (hyperplasia) and to an increase in the size of individual muscle fibres (hypertrophy). Myostatin may act in a threshold-dependent manner because reduction in protein level results in muscle hypertrophy but not in hyperplasia (Zhu *et al.*, 2000). Therefore, negative size control is an important tool in developmental biology, which functions independently of patterning control and can be executed by a diffusible factor.

Following the isolation of *Myostatin*, numerous groups have determined that breeds of cattle, including Piedmontese and Belgian Blue, which are characterised by excessive muscle development (Muscle doubling), harbour mutations in the coding region of the *Myostatin* gene (Kambadur *et al.*, 1997; McPherron and Lee, 1997). However, the developmental need to negatively regulate muscle size is not clear. Recent studies have detected *Myostatin* in tissues other than skeletal muscle, including the mammary gland and Purkinje fibres of the heart, which implies additional yet unexplored functions of Myostatin (Ji *et al.*, 1998; Sharma *et al.*, 1999). Interestingly, *Myostatin* is expressed in injured and regenerating muscle; patients suffering from AIDS-related muscle wasting show elevated serum levels of Myostatin (Gonzalez-Cadavid *et al.*, 1998; Kirk *et al.*, 2000; Sakuma *et al.*, 2000). However, the function of Myostatin in these pathological conditions remains to be determined.

Myostatin is expressed in muscle during embryonic, foetal, and at a very low extent in adult life (Lee and McPherron, 1999). The exact molecular mechanism of muscle growth inhibition is not exactly known. *In vitro* analysis has shown a repression of myoblast proliferation (Taylor *et al.*, 2001; Thomas *et al.*, 2000). It is not known whether Myostatin exerts the same activity on myogenic cells during different stages of development because the structure and cellular properties of muscle change considerably during embryonic, foetal, and neonatal life (Miller and Stockdale, 1986; Stockdale, 1992). Furthermore, the response of myogenic cells to a particular environmental cue might differ during successive stages of development.

All skeletal musculature of vertebrates, with the exception of some head muscles, originates from paraxial mesoderm (Christ and Ordahl, 1995). Cells of paraxial mesoderm form transient epithelial structures, called somites. As well as being the source of skeletal muscle, the somites of higher vertebrates also give rise to cartilaginous tissue, including vertebrae, ribs, and dorsal dermis. During somite development, somite cells are committed to their prospective fate dependent on their location within the somite and proximity to signals from adjacent tissues. Only cells of the dorsal half of the somites retain myogenic potential and reside within the epithelial dermomyotomal layer underneath the surface ectoderm. The ventral half of the somites deepithelialises and forms the sclerotome, the precursor of vertebrae and ribs.

Muscle cells are recruited only from the edges of the dermomyotome and form the myotome, which morphologically resembles a sheet of cells situated underneath the dermomyotome (Cinnamon *et al.*, 1999; Denetclaw and Ordahl, 2000; Huang and Christ, 2000; Kahane *et al.*, 1998). As dermomyotomal cells are recruited to form the myotome, the muscle differentiation programme is initiated by the expression of the myogenic regulatory factors *MyoD* and *Myf-5* (Pownall and Emerson, 1992). Initially, recruitment of myogenic precursors takes places mainly at the dorsomedial and ventrolateral edges of the dermomyotome, which enables dorsomedial (epaxial) and ventrolateral (hypaxial) elongation of the myotome (Cinnamon *et al.*, 1999; Denetclaw *et al.*, 2001; Huang and Christ, 2000; Ordahl *et al.*, 2001). It is not known why myotomal cells are recruited at these sites because experimental manipulations have shown that all cells of the dermomyotome can be instantaneously induced to form muscle. Although this leads to an initial thickening of the myotome, subsequent muscle development is impeded due to the depletion of the reservoir of proliferating muscle precursors (Amthor *et al.*, 1999). This suggests the existence of muscle inhibitor(s) that regulates the recruitment of dermomyotomal cells for myotomal development, ensuring a stable population of precursors which enables long-term growth of muscle.

At occipital and limb levels, small populations of cells delaminate from the ventrolateral edge of the dermomyotome and migrate into adjacent mesenchyme to form the skeletal muscle of the tongue and limbs (Chevallier *et al.*, 1977; Christ *et al.*, 1974; Huang *et al.*, 1999). After myogenic cells migrate into limb bud mesenchyme, they form premuscle masses that are situated at the dorsal and ventral aspects of the limb buds. Premuscle masses consist of subectodermally located undifferentiated, proliferating muscle precursors (marked by the expression of *Pax-3*) and differentiating muscle cells (marked by the expression of *MyoD*), which are situated more towards the mesenchymal centre of the limb (Amthor *et al.*, 1998). Only after having down-regulated *Pax-3* expression do myogenic cells initiate the differentiation programme. During initial limb outgrowth, premuscle masses simply enlarge by extension in all axes. From HH stage 28 onwards, however, premuscle masses split into individual blocks, and at HH stages 31–32, all different limb muscles are formed.

A previous study has analysed the expression of *Myostatin* in the chick by using RT-PCR, which generated temporal but no spatial data (Kocamis *et al.*, 1999). We therefore have carried out a temporospatial examination of the expression of chick *Myostatin* and present the first detailed profile of *Myostatin* expression during vertebrate development. Our work shows that the expression of *Myostatin* is initiated relatively late during somite development, i.e., a considerable time after the formation of the sclerotome, dermomytome, and myotome. *Myostatin* is expressed in the central part of the dermomyotome but not in the dorsomedial and ventrolateral lips. *Myostatin* was also detected in the subectodermal mesenchyme, the site of dorsal dermis precursors, and in the myotome. During late

embryonic stages, *Myostatin* is expressed in hypaxial but not in epaxial muscle. We show that, during limb development, *Myostatin* is initially expressed in myogenic cells and additionally in nonmyogenic cells of the mesenchymal core. *Myostatin* becomes localised to specific limb muscles only at late stages of embryonic development. To identify the environmental influences that regulate the expression of *Myostatin* and to identify the type of cells which express *Myostatin*, we performed a series of tissue manipulations, including removal of ectoderm, neural tube, notochord, and floor plate, and we determined the influence of Sonic hedgehog protein. Finally, we demonstrate that application of Myostatin protein to developing limb muscle leads to the down-regulation of *Pax-3*, *Myf-5*, and *MyoD*. The long-term effect of Myostatin is a decrease in the amount of terminally differentiated muscle.

MATERIALS AND METHODS

Preparation of Chick Embryos

Fertilised chicken eggs were incubated at 38°C, and the embryos were staged according to Hamburger and Hamilton (1992). Experiments were performed on embryos at stages 13–23, reincubated for a total of 3 days, sacrificed, and processed for whole-mount *in situ* hybridisation.

Myostatin and Sonic Hedgehog Bead Preparation

Recombinant Myostatin protein was purchased from R&D Systems. Sonic hedgehog (Shh) was a gift from Professor Andy McMahon (Boston, MA). All proteins were applied to 80- to 120-μm Affigel beads (Sigma). The proteins were loaded onto beads as described by Cohn *et al.* (1995). Myostatin was used at 0.3- to 1-mg/ml concentrations, and Shh was used at 8 mg/ml.

Bead Application and Microsurgical Procedures

For bead implantation, the dorsal ectoderm and mesenchyme of the right wing or somites were punctured with an electrolytically sharpened tungsten needle, and beads were inserted into the punctured mesenchyme by using a blunt glass needle. Beads were implanted at HH stages stated in the text.

For ectoderm removal, the ectoderm was stained with Nile Blue *in ovo* using a blunt glass needle coated with 2.5% agar containing 2% Nile Blue. The ectoderm was peeled from the mesenchyme immediately after staining. At thoracic level, ectoderm was removed from stage 19–20 embryos extending from somites at interlimb level and from the lateral side of the neural tube at a dorsomedial limit down to the abdominal wall at a ventrolateral limit. At limb level, ectoderm was removed from the dorsal and ventral limb surface avoiding the limb margins, apical ectodermal ridge, and the ectoderm overlying the zone of polarising activity of HH stage 22–23 embryos.

Portions of unilateral halves of neural tube were removed at the level of the segmental plate mesoderm as previously described (Christ *et al.*, 1992). Tissue extending over 8–12 prospective somite length was removed.

Notochord and floor plate were removed at the level of the segmental plate mesoderm by opening the neural tube along the dorsal midline with a tungsten needle. Thereafter, a cut was made on either side of the floor plate and the floor plate was removed together with the attached notochord. The open neural tube was closed by decreasing the surface tension, which was achieved by removing 2 ml of albumin from the egg.

The intermediate third of the dermomyotome was removed over the extent of four somites at HH stage 15–18 embryos. In a first step, ectoderm was incised and lifted from the dermomyotome, and in a second step, the intermediate dermomyotome was removed by using a tungsten needle and a mouth-operated micropipette. After tissue removal, the ectoderm was placed back in order to cover the operation site. No enzymes were used in neural tube, notochord, or dermomyotome removal.

For the generation of muscle-free limbs, somatic mesoderm of the prospective wing area was isolated together with the overlying ectoderm from quail embryos at HH stage 13–15. These wing anlagen were grafted into the laterally opened coelomic cavity of chick embryos at HH stages 15–17. After a reincubation period of 6–10 days, the host embryos were sacrificed, dissected, and processed for *in situ* hybridisation.

Whole-Mount in Situ Hybridisation

All chick embryos were washed in PBS and then fixed overnight in 4% paraformaldehyde at 4°C. Anti-sense RNA probes were labelled with digoxigenin, and whole-mount *in situ* hybridisation was performed as described by Nieto *et al.* (1996). The following probes were used in this study: *MyoD*, clone CMD9 full 1.5-kb length fragment (gift from Professor Bruce Patterson); *Myf-5*, a clone kindly provided by Dr. Antony Graham. *Pax-3*, 645-bp fragment corresponding to nucleotides 468-1113 (gift from Dr. Martin Goulding); chick *Myostatin*, 1-kb fragment was a kind gift from Professor Se Jin Lee; full-length *cLmx-1* (3 kb) was size reduced to 0.5-kb fragments by using alkaline hydrolysis as described by Nieto *et al.* (1996); *Lmx-1* was kindly provided by Dr, M. Ensini; full-length *cTbx-5* was kindly provided by Professor J. C. Izpisua Belmonte. Whole-mount embryos were cryosectioned for further histological examination.

Immunohistochemistry on Whole Mounts for the Detection of Desmin

Embryos were fixed overnight in 4% paraformaldehyde (PFA), dehydrated into 100% methanol, incubated for 1 h in 4:1 methanol/H_2O_2 (6% final), washed in PBT (PBS containing 0.5% Triton). Embryos were treated in Proteinase K (10 μg/ml) and after a wash in PBT, fixed in 4% PFA for 20 min. Following a brief wash in PBT, embryos were incubated for 1 h in 10% horse serum (in PBT) and then overnight with anti-Desmin monoclonal antibody (DAKO, 1:500, in horse serum/PBT). Embryos were extensively washed in PBT and then incubated overnight in secondary antibody (alkaline phosphatase-conjugated goat anti-mouse Ig antibody; Sigma, 1:500, in horse serum/PBT). Subsequently, embryos were washed in PBT, transferred in NTBT buffer (Nieto *et al.*, 1996), incubated for 5–10 min in colour reagent (4.5 μl NBT and 3.5 μl BCIP in 1 ml NTBT-buffer; Boehringer–Mannheim), washed in NTBT buffer, cleared in dimethylformamide, and stored in 4% PFA.

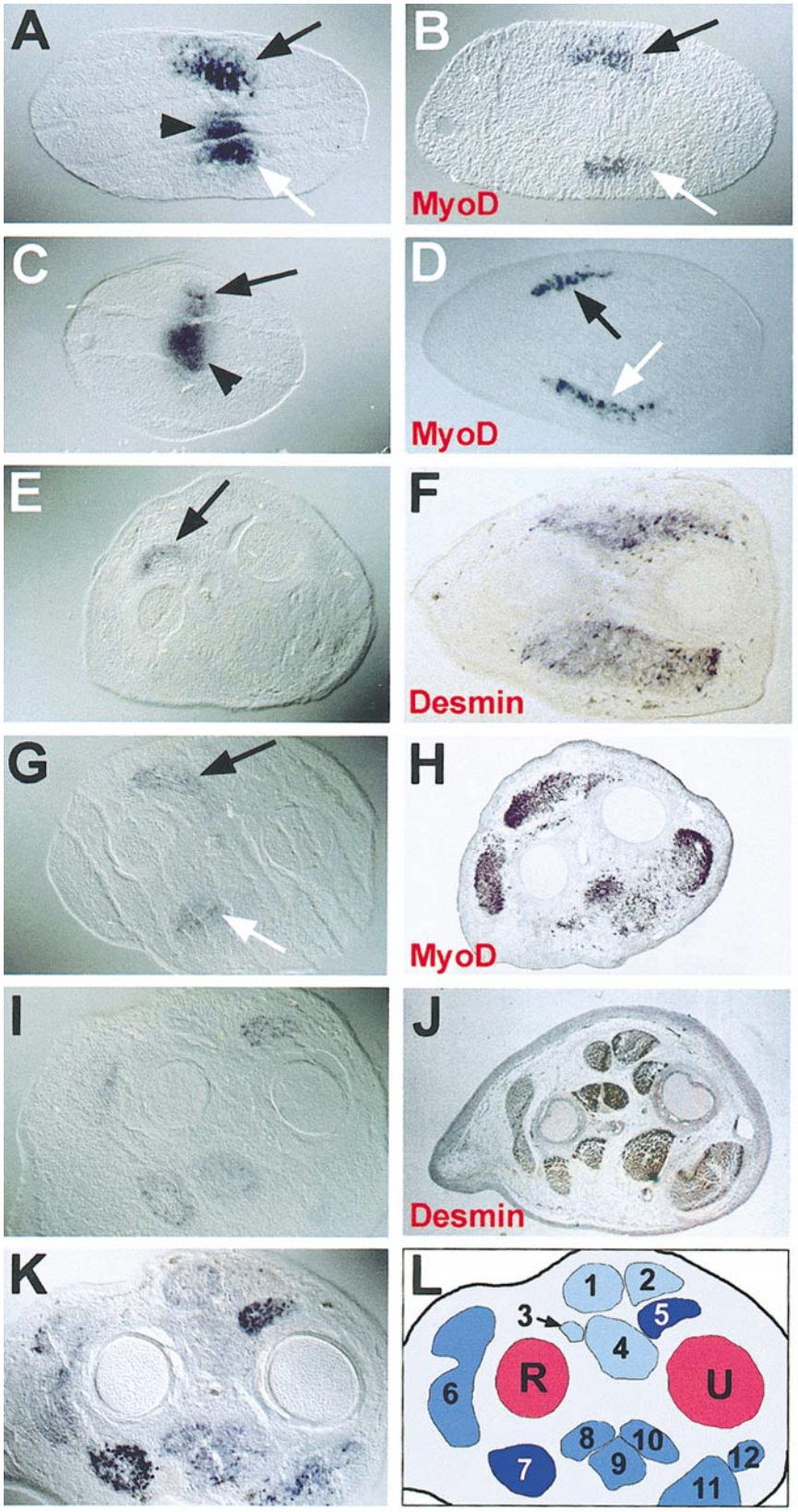

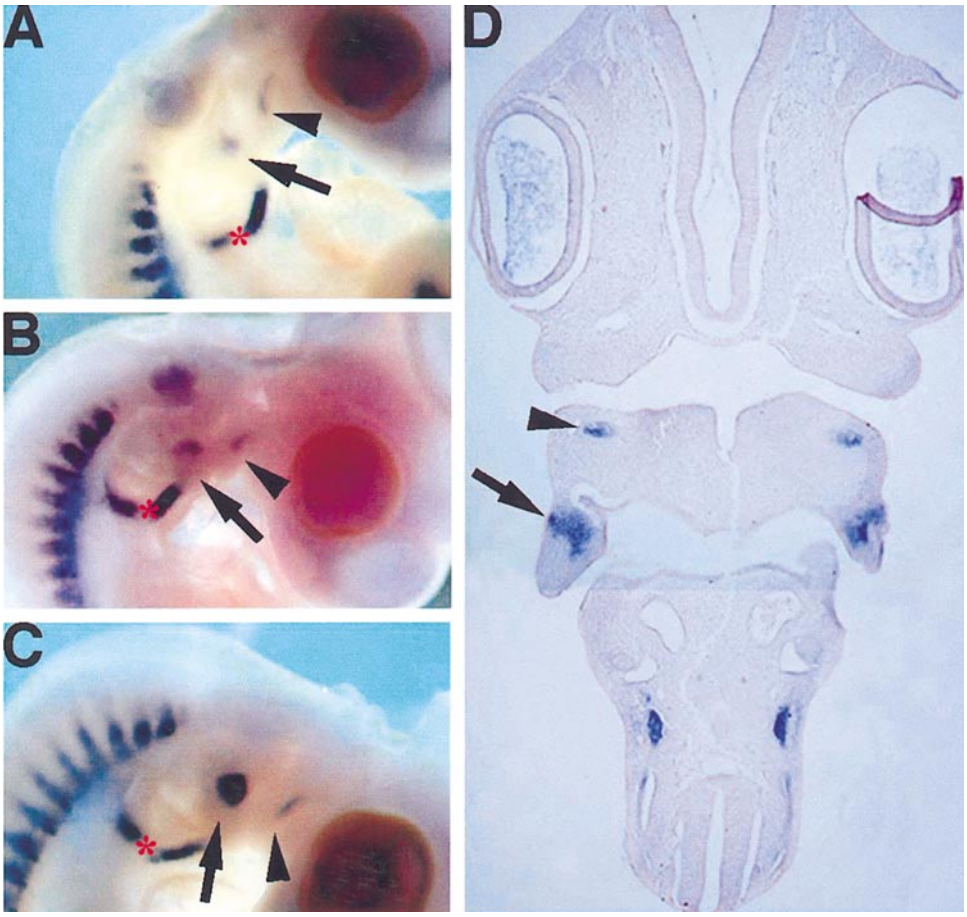

FIG. 4. Myostatin expression during head development. Red asterisk marks hypoglossal cord. (A) At HH stage 21, faint expression of *Myostatin* is detectable in branchial arch 1 (arrowhead) and branchial arch 2 (arrow). (B) By HH stage 22, *Myostatin* expression in both branchial arch 1 (arrowhead) and 2 (arrow) is evident at the proximal aspect. (C) By HH stage 23, the broad strong patch of expression in branchial arch two (arrow) contrasts the faint bar of expression in branchial arch one (arrowhead). (D) Frontal section of HH stage 23 head shows *Myostatin* expression in branchial arch 1 confined to the mesenchymal core (arrowhead) and contrasts the expression in branchial arch 2, which extends up to the ectoderm (arrow).

FIG. 3. Tissue expression of *Myostatin* and muscle markers during wing bud development. All wing buds depicted following transverse sectioning. (A) *Myostatin* expression in a dorsal (black arrow) and ventral mesenchymal position (white arrow) corresponding to *MyoD* expression of dorsal (black arrow) and ventral premuscle masses (white arrow) in (B) of an HH stage 22 wing bud. Additional *Myostatin* expression domain in the mesenchymal core (black arrowhead, in A). (C) *Myostatin* expression in the mesenchymal core of an HH stage 25 wing bud (arrowhead). Expression declines in the dorsal premuscle (arrow) and is down-regulated ventrally compared with the *MyoD* expression of dorsal (black arrow) and ventral premuscle masses (white arrow) in (D). (E) *Myostatin* expression in a small dorsal muscle domain (arrow) at HH stage 28 compared with Desmin expression, which marks ventral and dorsal muscle in (F). (G) Myostatin expression in a small dorsal (black arrow) and ventral muscle domain (white arrow) at HH stage 30. (H) At HH stage 29, zeugopod muscle splitting is well in progress as shown by *MyoD* expression. (I–K) Different levels of *Myostatin* expression in different zeugopod muscles of an HH stage 31 wing (I) and HH stage 32 wing (K) compared with the muscle pattern after Desmin staining (J). Note heterogeneous *Myostatin* expression within single muscles. (L) Diagrammatic representation of (K) shows muscles with high Myostatin expression in dark blue, low expression in medium blue, and no expression in light blue. Radius (R) and ulna (U). (1) Anconeus, (2) extensor digitorum communis, (3 and 4) entepicondyloulnaris, extensor medius longus, extensor indicis longus, (5) extensor metacarpi ulnaris, (6) extensor metacarpi radialis, (7) pronator superficialis, (8) pronator profundus, (9 and 10) flexor digitorum profundus, and (11 and 12) flexor carpi ulnaris muscles.

RESULTS

Expression of Myostatin during Chick Somite Development

Expression of *Myostatin* was first detected by whole-mount *in situ* hybridisation in HH stage 15 chick embryos with transcripts localised in the ventrolateral portion of the four to five most rostrally situated somites (Fig. 1A). Additionally, faint expression was found throughout somites I-II and in the tail bud. By HH stage 17, *Myostatin* transcripts were no longer detectable in the caudal region of the embryo (Fig. 1B). Rostrally, the expression was found in the ventrolateral portion of all occipital and cervical somites. *Myostatin* expression was also detected in the prospective tongue muscle-forming region from HH stage 17 onwards (Figs. 1B–1E). At HH stage 19, faint expression was additionally detected in somites at interlimb level (Fig. 1C). At stage 20, all but the most caudal somites expressed *Myostatin*, which nevertheless eventually up-regulated the gene at later stages (Figs. 1D–1H). In addition to the expression in the centre of the dermomyotome, a line of expression was present at the ventral side of somites, which corresponded to cells situated next to the hypaxial bud of the dermomyotome, intermediate mesoderm, and at the endodermal plicae of the coelomic cavity (Figs. 1D, 2A, and 2B). Transverse sections at the thorax level of HH stage 20 embryos revealed strong *Myostatin* expression in the centre of the dermomyotome, which extended dorsomedially and ventrolaterally during later stages (Figs. 2A and 2C). Expression was never detected in the dorsomedial or ventrolateral dermomyotomal lips. In somites at thorax level of HH stage 22 embryos, *Myostatin* expression in the dermomyotome extended to the ectoderm, thus, into a region which forms the dermis of the back later in development (Fig. 2C). Additionally, transverse sections of somites at thorax level of HH stage 22 embryos revealed a differential expression of *Myostatin* in the myotome along its craniocaudal axis. The centre of the myotome did not express *Myostatin* (Fig. 2C), whereas expression was found in the rostral and caudal part of the myotome (Figs. 2D and 2F). At stage 25, *Myostatin* expression was found in the dermomyotome and in the hypaxial part of the myotome, and additionally in the dorsomedial tip of the myotome (Fig. 2E). At later stages, dermomyotomal expression was down-regulated, and at HH stage 30, *Myostatin* expression was found only in hypaxial muscle (Figs. 1I and 1J).

Therefore, *Myostatin* expression was detected relatively late during somite development, well after compartmentalisation of the somite in its derivatives, dermomyotome, myotome, and sclerotome. Strong expression was detected in the intermediate portion of the dermomytome and myotome as well as in prospective subectodermally located dermal cells.

Myostatin Expression during Limb Development

In the limbs, *Myostatin* expression was first detected in a small proximomedial domain in both wing and leg buds at HH stage 21, which extended distally during development (Figs. 1E–1H). Transverse sections of wing buds at HH stage 22 revealed that the expression was composed of three mesenchymal domains (Fig. 3A). One was dorsally situated and corresponded approximately to the *MyoD* expression domain of the dorsal premuscle mass (Figs. 3A and 3B). The second was ventrally situated and corresponded approximately to the *MyoD* expression domain of the ventral premuscle mass (Figs. 3A and 3B). These muscle related expression domains were down-regulated during the following stages compared with the *MyoD* expression of premuscle masses at HH stage 25 (Figs. 3C and 3D). The third more centrally located expression domain corresponded approximately to the mesenchymal core of the limb bud and was present up to HH stage 28 (Figs. 3A and 3C). *Myostatin* was reexpressed in limb muscle from HH stage 28 onwards and was first detected at low levels of transcripts in proximal limb muscle (data not shown). Additionally, we detected a small expression domain dorsal to the radius that represented a part of the zeugopod muscle when compared with Desmin expression at this stage (Figs. 3E and 3F). At HH stage 29, zeugopod muscle started to split into individual muscles as shown by the expression of *MyoD* (Fig. 3H). At HH stage 30, a small *Myostatin* expression domain was detected in the ventral limb muscle in addition to the small dorsal expression domain (Fig. 3G). However, these expression domains could not be correlated to specific muscles. From HH stage 31 onwards, expression became confined to individual muscles (Fig. 3I). Remarkably, only some muscles expressed *Myostatin*, and the level of expression differed between individual muscles compared with the Desmin expression, which marks all muscle at HH stage 32 (Figs. 1K and 1L, and 3J–3L). Only pronator superficialis and extensor metacarpi ulnaris muscles expressed *Myostatin* at high levels. Extensor metacarpi radialis, pronator profundus, flexor digitorum profundus, flexor digitorum superficialis, and flexor carpi ulnaris muscles expressed *Myostatin* at low level and remaining muscles showed almost no expression. Moreover, even within single muscles there was heterogeneity in expression (Figs. 3K and 3L). In summary, *Myostatin* was initially expressed in limb mesenchyme in both myogenic and nonmyogenic regions. During late limb bud stages, *Myostatin* expression was found within specific muscles.

Expression of Myostatin during Head Development

Development of the head muscle differs from that of the body in terms of its origin and the molecular pathways for its differentiation (Mootoosamy and Dietrich, 2002). Head muscle does not develop from somites but originates primarily from head mesoderm (Wachtler and Jacob, 1986). Additionally, head muscle does not express *Pax-3* (Franz *et al.*, 1993; Tajbakhsh *et al.*, 1997).

Expression of *Myostatin* in the head became detectable at HH stage 20 and was clearly evident at HH stage 21 with two zones of expression: a bar of transcripts in the branchial arch one and a patch of expression in brachial arch two (Fig. 4A). One stage later and following further outgrowth of the branchial arches, it became evident that the expression of *Myostatin* was more pronounced at the proximal aspect and did not extend to the distal margins (Fig. 4B). By HH stage 23, the broad strong patch of expression in branchial arch two contrasted the faint bar of expression in branchial arch one (Fig. 4C). Frontal sections revealed that the expression in branchial arch one was confined to a central portion of the mesenchyme, whereas in branchial arch two, mesenchymal expression extended to the ectoderm (Fig. 4D). *Myostatin* expression was not detected in any other branchial arch. Therefore, the *Myostatin* expression pattern in the head was related to the identity of the branchial arch. In addition, expression of the gene was found in both the central and subectodermal mesenchyme.

Regulation of Myostatin Expression in the Somites

Somite development, and in particular determination and differentiation of somite-derived cell lineages, depends on signals which emanate from neighbouring tissues. In this section, we examined whether *Myostatin* expression in somites relies on extrinsic signalling and whether *Myostatin*-expressing cells belong to specific somite-derived cell lineages. In the first set of experiments, we determined the influence of the ectoderm as we have previously shown that this tissue maintains *Pax-3* expression in the dermomytome (Amthor *et al.*, 1999). We removed trunk ectoderm only on the right side of HH stage 19–20 embryos and found a down-regulation of *Myostatin* expression on the operated side 26 h after operation ($n = 6$, Fig. 5A). The dorsomedial–ventrolateral extension of the dermomyotome was shortened on the operated side compared with contralateral (Fig. 5B). At the unoperated side, *Myostatin* expression was found predominantly in the dermomyotome, subectodermal mesenchyme, and myotome. After ectoderm removal, however, *Myostatin* expression was lost in all locations except a central domain that corresponded to the central part of the myotome (Fig. 5B). Therefore, ectodermal signalling sustains dermomyotomal expression of *Myostatin*, but expression in the myotome does not rely on this tissue.

Application of Shh to the mature somites has been shown to transiently induce muscle differentiation at the expense of the proliferating *Pax-3*-expressing myogenic precursors (Amthor *et al.*, 1999). We implanted Shh beads to the right side of the trunk at HH stages 18–19 embryos prior to the onset of *Myostatin* expression in somites ($n = 9$). Following a reincubation of 12 h, embryos developed to HH stage 21 and expressed *Myostatin* in the central part of the dermomyotome and subectodermal mesenchyme on the unoperated left side (Figs. 5C and 5D). Exposure to Shh on the right side of the trunk resulted in complete lack of *Myostatin* expression on the operated side (Figs. 5C and 5D). Subsequently, we implanted Shh beads in the trunk of embryos at HH stage 20 ($n = 4$) for a period of 31 h (embryos developed to HH stage 26). On the unoperated left side, *Myostatin* expression resided in the ventral part of the myotome (Figs. 5E and 5F). Interestingly, on the operated side, *Myostatin* expression was now up-regulated. The expression domain was enlarged and corresponded to an enlarged ventral part of the myotome (Figs. 5E and 5G).

We performed ablation experiments that complimented the application of Shh. We tested whether *Myostatin* expression in somites depends on Shh signalling and removed notochord and floor plate (which both express Shh) prior to somite formation at prospective thorax level of HH stage 11–13 embryos ($n = 9$). Forty-eight hours after operation, embryos developed to HH stages 21–23. We found that without a floor plate and notochord, somites at the site of operation appeared considerably smaller than in unoperated embryos (Fig. 5H). Furthermore, somite-derived structures (dermomyotome, myotome, and sclerotome) could not be morphologically identified (Fig. 5I). Despite this, we found strong *Myostatin* expression at the site of operation that extended ventrally to a position where the sclerotome would normally develop (Fig. 5I). Furthermore, expression was considerably up-regulated in somites at the site of operation compared with adjacent unoperated regions. Therefore, notochord and floor plate, which both are tissues that express Shh, inhibit *Myostatin* expression.

The dorsomedial part of the dermomyotome gives rise to epaxial muscle and its development depends on neural tube signalling (Bober *et al.*, 1994; Rong *et al.*, 1992). In the next experiment, we determined whether the expression of *Myostatin* in the dermomyotome depends on neural tube signals by ablating the right half of the neural tube prior to somite formation at prospective thorax level of HH stage 13–14 chick embryos ($n = 4$). Two days after unilateral neural tube ablation, somite tissue was much smaller on the operated side compared with the unoperated left side (Fig. 5J). The somite tissue was morphologically well differentiated into dermomyotome, myotome, and sclerotome. However, even though the dermomyotome and the myotome were shortened in their dorsomedial-to-ventrolateral extension, we found strong *Myostatin* expression in the remaining dermomyotome, and the size of the expression domain was only slightly smaller than on the unoperated left side. This experiment suggests that only a minority of *Myostatin*-expressing cells depends on neural tube signalling and that the majority of *Myostatin*-expressing cells are confined to the hypaxial and not to the epaxial somite domain.

Regulation of Myostatin Expression in the Limb

Limb ectoderm sustains proliferation in subectodermal mesenchyme and inhibits muscle differentiation and chondrogenesis (Amthor *et al.*, 1998; Solursh and Reiter, 1988). We determined the influence of the ectoderm on *Myostatin*

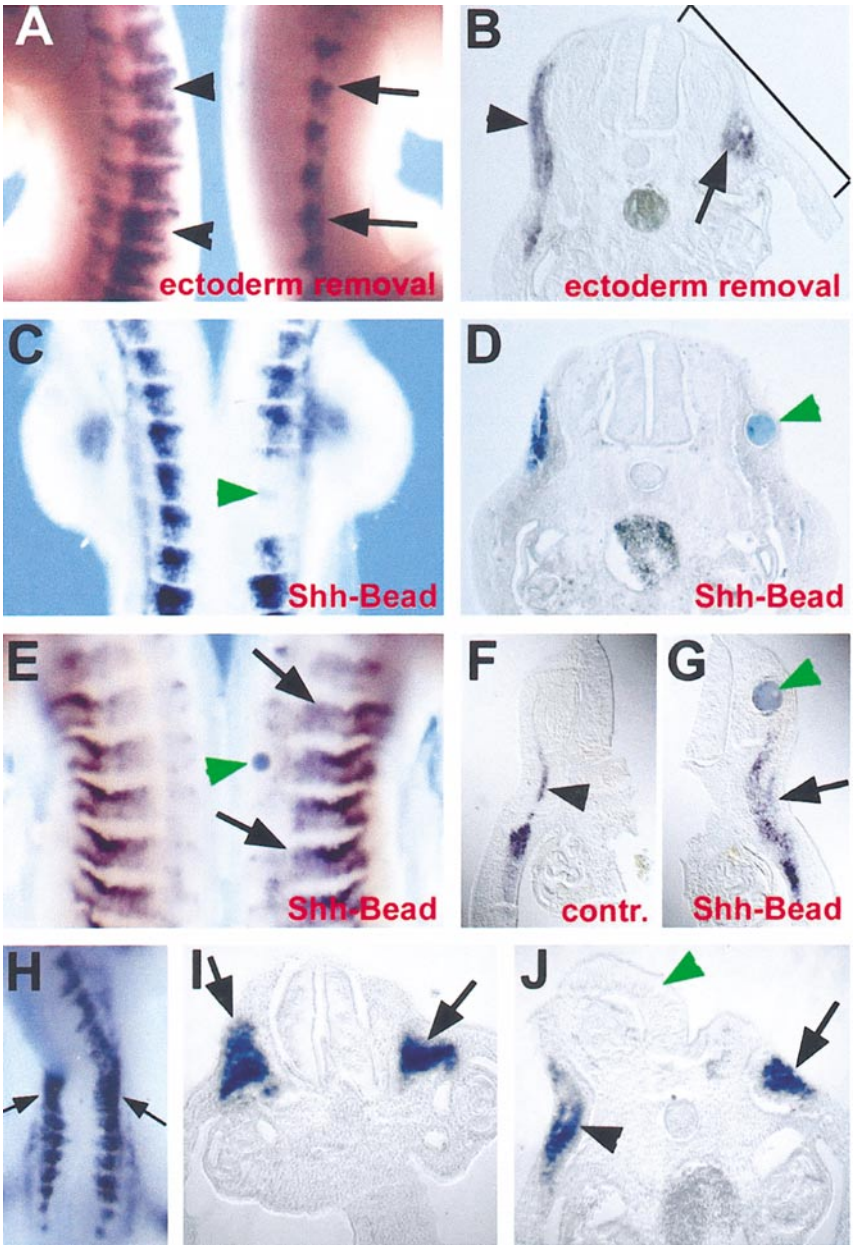

FIG. 5. Regulation of *Myostatin* expression during somite development. (A) One day after removal of trunk ectoderm, *Myostatin* expression in somites is shortened in the mediolateral extension (arrows) compared with the unoperated left side (arrowheads). (B) Transverse section of whole mount shown in (A). On the unoperated left side, expression is found in the dermomyotome and myotome (arrowhead), whereas on the operated side, only the central part of the myotome expresses *Myostatin* (arrow). Bracket marks extension of ectoderm removal. (C, D) Twelve hours after exposure to Shh, *Myostatin* expression is completely down-regulated in the dermomyotome near the implanted bead (green arrowhead) compared with the unoperated left side. (E) Thirty-one hours after exposure to Shh, *Myostatin* is reexpressed, and somites appear enlarged (arrows). Bead (green arrowhead). (F, G) Transverse section of (E) reveals that the ventral part of the myotome, which expresses *Myostatin*, is enlarged (G, arrow) compared with the unoperated left side (F, arrowhead). Bead (green arrowhead). (H) Two days after removal of floor plate and notochord, the embryo developed a significant scoliosis at the operation site, but *Myostatin* is still strongly expressed in the somites (arrows). (I) Transverse section at the operation site of the whole mount shown in (H) reveals ventral extension of the *Myostatin* expression domain in lack of floor plate and notochord signalling compared with Fig. 2A. The somite tissue is smaller, and a dermomyotome, myotome, and sclerotome cannot be morphologically identified (arrows). (J) After removal of the right half of the neural tube, the ipsilateral somite tissue is smaller but well differentiated in dermomyotome, myotome, and sclerotome. The dermomyotome highly expresses *Myostatin* (arrow). The expression domain is only slightly smaller compared with the unoperated left side (arrowhead). Remaining half of neural tube (green arrowhead).

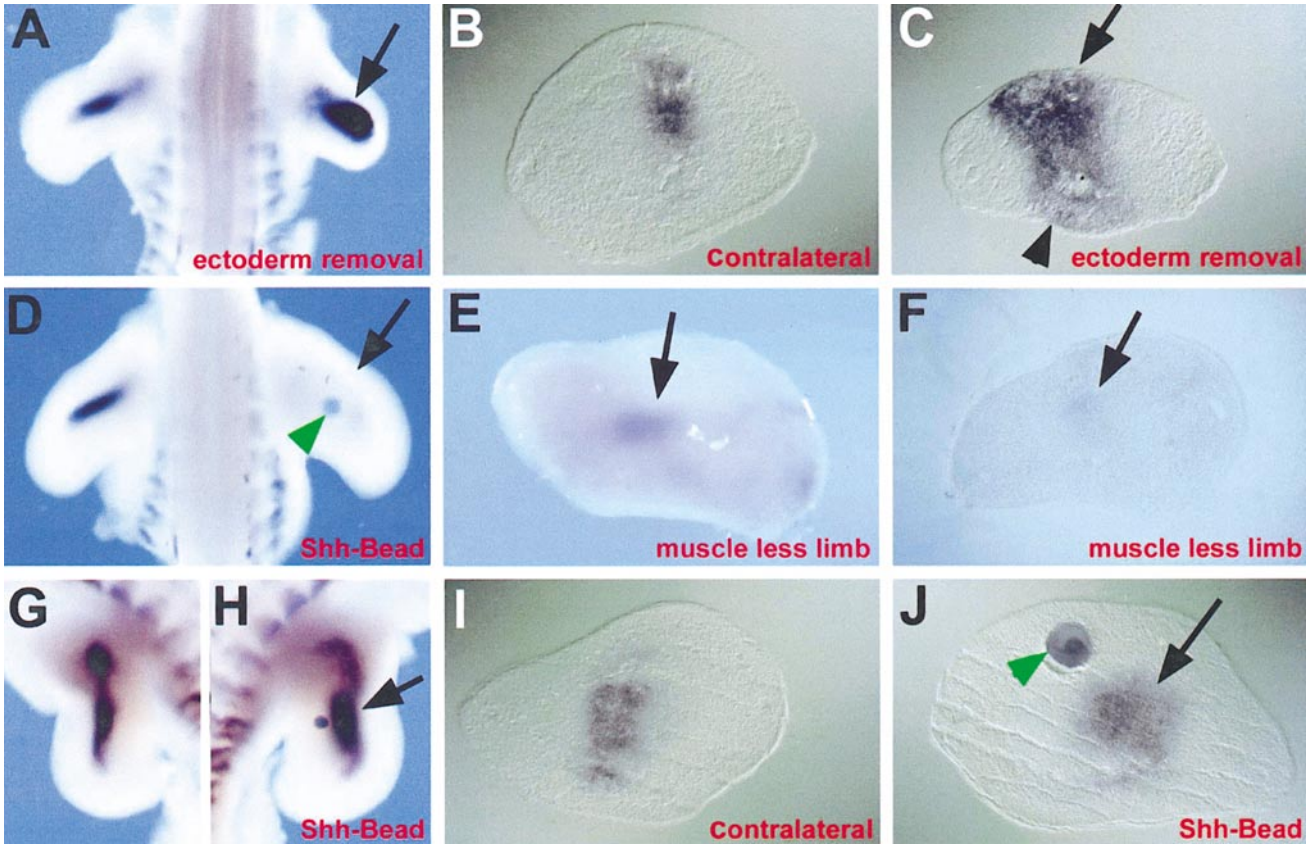

FIG. 6. Regulation of *Myostatin* expression during limb muscle development. (A) Up-regulation of *Myostatin* expression (arrow) after removal of dorsal and ventral wing ectoderm, although the size of the wing appears smaller compared to the unoperated left wing. (B, C) Transverse sections of wing buds shown in (A). Extension of the *Myostatin* expression domain to the dorsal (arrow) and ventral subectodermal mesenchyme (arrowhead) after ectoderm removal (C) compared with the expression in the mesenchymal core of the unoperated left wing (B). (D) Complete down-regulation of *Myostatin* 22 h after Shh bead implantation (arrow) compared with the unoperated left wing. Bead (green arrowhead). (E) Wing bud, which failed to be populated with muscle after heterotopic development, still expresses *Myostatin* in a central domain (arrow). (F) Transverse section of the whole mount shown in (E) reveals a faint *Myostatin* expression in the mesenchymal core (arrow). (G, H) Thirty-one hours after Shh bead implantation, the *Myostatin* expression domain (arrow) and the whole wing bud enlarged (H) compared with the unoperated left side (G). (I, J) Transverse sections of wings shown in (G) and (H) reveals that the *Myostatin* expression domain in the mesenchymal core enlarged (arrow), but there is no ectopic expression (J) compared with the unoperated left wing (I). Bead (green arrowhead).

expression and ablated the right wing ectoderm from both the dorsal and ventral surfaces at HH stage 22–23 ($n = 7$). Care was taken not to damage the distal ectoderm, thereby maintaining apical ectodermal ridge and progress zone integrity. Following a reincubation period of 13 h, we observed a dramatic increase in *Myostatin* expression, although operated wings appeared smaller than unoperated left wings (Fig. 6A). Transverse sections revealed that not only was the *Myostatin* expression more intense than normal, but that the domain of expression had expanded in both the dorsoventral and anteroposterior axes (Figs. 6B and 6C). *Myostatin* expression extended to the operated surface following ectoderm removal compared with the normal expression at this stage in the unoperated left wing, which is only confined to the mesenchymal core. Therefore, during early limb bud development, expression of *Myostatin* in subectodermal regions is inhibited by limb ectoderm.

Sonic hedgehog (Shh) has been previously shown to act synergistically with limb ectoderm to maintain *Pax-3*-linked proliferation of limb muscle precursors and to prevent precocious muscle differentiation (Amthor *et al.*, 1998; Duprez *et al.*, 1998). Implantation of beads soaked in Shh in wing bud mesenchyme at HH stage 20 resulted in a complete down-regulation of *Myostatin* expression 20 h after operation compared with the unoperated left wing ($n = 11$, Fig. 6D). Operated wings were enlarged compared with the unoperated wings. However, longer reincubation (31 h, $n = 4$) resulted not only in the reappearance of *Myostatin* expression in the operated wings, but the expression domain was enlarged (Figs. 6G and 6H). Transverse sections

revealed that the enlarged *Myostatin* expression domain still resided in the mesenchymal centre of the enlarged operated wing compared with the unoperated wing (Figs. 6I and 6J).

We were intrigued by the expression of *Myostatin* in the central region of the limb bud that is not populated by myogenic cells. We grafted the prospective wing-forming region into the coelomic cavity before myogenic cells migrated into wing bud mesenchyme. Such operation results in the development of muscle free wings (Christ *et al.*, 1977). Wing buds were grown until they reached a stage equivalent to HH stage 25. We show that heterotopically developed wings expressed *Myostatin* in the normal central domain, but the intensity of expression was much weaker than in normal wings (Figs. 6E and 6F; compare with the unoperated left wing in Figs. 6A and 6B).

Effect of Myostatin Protein on Limb Muscle Development

We explored the function of Myostatin during muscle development and implanted beads soaked in *Myostatin* into the dorsal subectodermal mesenchyme of right wings of HH stage 21–22 embryos and analysed the expression of the myogenic marker genes *Pax-3*, *Myf-5*, *MyoD*, and Desmin at various intervals thereafter. Beads were implanted in the centre of the dorsal premuscle mass at HH stage 21, when *Pax-3*, *Myf-5*, and *MyoD* expression has already been established (Amthor *et al.*, 1998; Delfini *et al.*, 2000). Implantation of beads soaked in 1 mg/ml Myostatin resulted in a down-regulation of the expression of *Pax-3*, *Myf-5*, and *MyoD* within 6 h following operations compared with the unoperated left wings (*Pax-3*, $n = 4$; *Myf-5*, $n = 5$; *MyoD*, $n = 6$; Figs. 7A, 7C, and 7E). Down-regulation of these genes occurred predominantly in the dorsal premuscle masses, especially in the proximity of the beads and to a considerably lower extent (if at all) in the ventral premuscle masses. The presence of Myostatin beads did not completely stop further development of premuscle masses as the expression domains of *Pax-3*, *Myf-5*, and *MyoD* enlarged following 24 h after operation compared with 6 h after operation. Significantly, however, the total size of the expression domains were smaller compared with the unoperated left wings ($n = 7$ for *Pax-3*; $n = 3$ for *Myf-5*; $n = 12$ for *MyoD*; Figs. 7B, 7D, and 7F). Furthermore, at the site of the implanted beads, there was a lack of *Pax-3*, *Myf-5*, and *MyoD* expression. Finally, we tested whether the effect of Myostatin decreasing the transcription of *Pax-3*, *Myf-5*, and *MyoD* impairs muscle growth. We implanted beads soaked in 1 mg/ml Myostatin at HH stage 21 and analysed the expression pattern of Desmin 72 h after operation ($n = 5$). After this interval, beads were approximately located at the elbow joint. In most cases, the stylo- and zeugopodium appeared shortened. We found a considerable lack of desmin expression of dorsal stylopod, zeugopod, and autopod muscle in all cases examined. Even in cases in which overall limb outgrowth appeared normal, dorsal zeugopod and autopod muscles were almost completely abolished (Fig. 7G). Interestingly, as for *Pax-3*, *Myf-5*, and *MyoD* expression, ventral muscle did not seem to be affected when Myostatin beads were implanted on the dorsal side of the developing wing. Since Myostatin beads were implanted at HH stage 21 wing buds, thus, approximately 24 h before the onset of Desmin expression (HH stage 25 during normal development), it seems likely that Myostatin effects Desmin expression indirectly and via the down-regulation of *Pax-3*, *Myf-5*, and *MyoD* expression rather than having a direct effect.

We next analysed whether Myostatin acts concentration-dependent on myogenic cells and applied beads soaked in 0.33 mg/ml Myostatin to wing buds similar to above experiments. Exposure to low Myostatin concentration still resulted in a down-regulation of *Pax-3* and *MyoD* expression 1 day after bead implantation (*Pax-3*, $n = 5$; *MyoD*, $n = 5$; data not shown). However, the effect was less obvious and the range of down-regulation shorter compared with the effect of high concentrated Myostatin. Thus, Myostatin acts concentration-dependent on myogenic cells.

We analysed whether the effect of Myostatin on myogenic cells is specific and tested the expression of *Tbx-5* and *Lmx-1*, markers for wing mesenchyme and dorsal limb mesenchyme, respectively ($n = 4$ for *Tbx-5*, $n = 3$ for *Lmx-1*). Twenty-four hours after Myostatin bead implantation into the right wings, there was no difference in the expression of either gene compared with the unoperated left wings (data not shown). Thus, the effect of Myostatin on *Pax-3*, *Myf-5*, and *MyoD* expression seems to be specific and not caused by unspecific cell toxicity. Implantation of beads soaked in PBS only, into right wing buds of HH stage 21 embryos, did not change the expression of *Pax-3*, *MyoD*, and Desmin compared with unoperated left wings, nor did control beads change the ultrastructure of the mesenchyme (Amthor *et al.*, 1998, 2002).

In summary, Myostatin decreases expression of *Pax-3* and *Myf-5*, genes which are associated with the proliferation of myogenic cells (Amthor *et al.*, 1998; Delfini *et al.*, 2000). Furthermore, Myostatin also decreases expression of *MyoD*, which is associated with the onset of muscle differentiation. Such negative effect on the gene expression of key myogenic determinants eventually results in a deficit of terminally differentiated muscle.

DISCUSSION

Myostatin is a diffusible growth factor, which functions to limit the size of the musculature during growth of the organism (Lee and McPherron, 1999). In absence of Myostatin, the organism develops hypertrophy and hyperplasia of skeletal muscle (McPherron *et al.*, 1997; McPherron and Lee, 1997). The intriguing property of Myostatin to restrict muscle size without influencing positioning and patterning of muscle led us to determine the exact pattern and regulation of *Myostatin* expression and the effect of Myostatin protein during embryonic development.

Myostatin and Myotome Development

Axial muscle development begins with the involution of differentiating muscle cells of the dermomyotome, which forms the segmentally organised muscle anlagen of the trunk, called the myotomes. Although myotomal cells are recruited from all edges of the dermomyotome, it is thought that the dorsomedial and ventrolateral edges (synonyme lips) exert highest growth activity for myotome formation (Cinnamon *et al.*, 1999; Denetclaw *et al.*, 1997, 2001; Denetclaw and Ordahl, 2000; Ordahl *et al.*, 2001; Kahane *et al.*, 2001). This is reflected by a strong expression of *Pax-3* and a high rate of proliferation at these sites (Amthor *et al.*, 1999). We show that expression of *Myostatin* begins after somites are differentiated in dermomyotome, myotome, and sclerotome—not before HH stage 19 at the thoracic level. *Myostatin* is initially strongly expressed in the dermomyotome but excluded from the dorsomedial and ventrolateral dermomyotomal lips. Thus, *Myostatin* is not expressed at stages and sites that would interfere with the qualitative development of the myotome. The expression of *Myostatin* in the centre of the dermomyotome suggests that it reduces participation of expressing cells in myotome formation and therefore prevents hyperplasia. However, it is not that cells of the intermediate third of the dermomyotome cannot participate in muscle development. Huang and Christ (2000) followed the fate of intermediate dermomyotomal cells and found that they contribute to the hypaxial myotome. Therefore, cells, which express *Myostatin*, are biased towards the hypaxial lineage. This conclusion is reinforced by data from the somite manipulation experiments: lack of neural tube signalling results in epaxial muscle failing to form (Bober *et al.*, 1994; Christ *et al.*, 1992; Rong *et al.*, 1992). We show that, after neural tube removal, the size of the *Myostatin* expression domain is only slightly reduced. Thus, the majority of *Myostatin*-expressing cells are confined to the hypaxial somite domain. This becomes evident at later stages at which *Myostatin* expression is found in hypaxial but not in epaxial muscle of the trunk.

We previously have shown that trunk ectoderm maintains proliferation of dermomyotomal cells (Amthor *et al.*, 1998). Here, we show that dermomyotomal but not myotomal *Myostatin* expression depends on ectoderm signalling. Thus, it appears that *Myostatin*-expressing cells of the dermomyotome are linked to proliferation, whereas *Myostatin*-expressing cells of the myotome are postmitotic. We also have previously shown that treatment of mature somites with Shh results in a transition of dermomyotomal-located *Pax-3*-expressing cells into precocious *MyoD* expression, which expands the myotome. The switch from losing dermomyotomal identity to expressing myotomal marker occurs within 12 h after Shh treatment (Amthor *et al.*, 1998). These results are compatible with the finding of our present study because dermomyotomal-expressed *Myostatin* is lost within the same time period (12 h) after Shh treatment. Interestingly, although Shh treatment results in a loss of dermomyotomal *Myostatin* expression, there was no immediate up-regulation of *Myostatin* in the myotome in contrast to the precocious up-regulation of *MyoD* after the same procedure. However, *Myostatin* expression was up-regulated after an extended period following Shh exposure and marked the expanded myotome. Notochord and floorplate express *Shh* (Marti *et al.*, 1995). After removal of both structures, dermomyotomal markers expand ventrally because ventrally located somite cells are not induced to form sclerotome-derived structures (Amthor *et al.*, 1996; Christ *et al.*, 2000). We show that, after notochord and floorplate removal, *Myostatin* expression extends ventrally, which indicates that *Myostatin* expression marks cells of dorsal somite identity. Thus, during somite development, *Myostatin* is expressed in defined somite compartments, but the timing of *Myostatin* expression in these compartments was not experimentally altered.

We observed that the expression of *Myostatin* in the dermomyotome extends to the ectoderm. Thus, *Myostatin* is expressed in cells, which will form part of the dermis of the back. This is interesting as only a few genes, e.g., *Dermo-1* and *Frizzled-1*, have been found to be expressed in early stages of dermis development (Li *et al.*, 1995; Schmidt *et al.*, 2000). The subectodermal expression of *Myostatin* at this site could simply be "passive," i.e., a vestige of the expression found in the precursor cell type, which is derived from the dermomyotome. A more interesting hypothesis would be the active involvement of Myostatin in dermis formation. Myostatin, which we have shown to prevent muscle differentiation, could permit cells to adopt a dermis fate. In fact, in *Myf-5*$^{-/-}$ mice, cells, which normally would differentiate in muscle, are specified to form dermis or cartilage (Tajbakhsh *et al.*, 1996). Although dermis defects were not reported in *Myostatin*$^{-/-}$ mouse (McPherron *et al.*, 1997), dermis can originate from multiple sources (Christ and Ordahl, 1995; Le Lievre and Le Douarin, 1975; Olivera-Martinez *et al.*, 2000). Future work will investigate this hypothesis of dermis development.

Myostatin and Limb Muscle Development

Myostatin expression was detected in both myogenic and nonmyogenic regions during limb outgrowth. *Myostatin* expression resides at positions where *MyoD*-expressing cells of dorsal and ventral premuscle masses are localised and at a position where chondrogenic cells are found (Amthor *et al.*, 1998; Mallein-Gerin *et al.*, 1988). However, expression in myogenic regions is down-regulated at approximately HH stage 23 and only reappears at HH stage 28. At this stage, splitting of proximal muscle is well underway. Thus, it appears that *Myostatin* expression is not related to muscle patterning and that the onset of expression follows the splitting of muscle and not vice versa.

Removal of limb ectoderm results in a dramatic decrease in mitotic levels in the subectodermal mesenchyme (Amthor *et al.*, 1998). However, following an identical

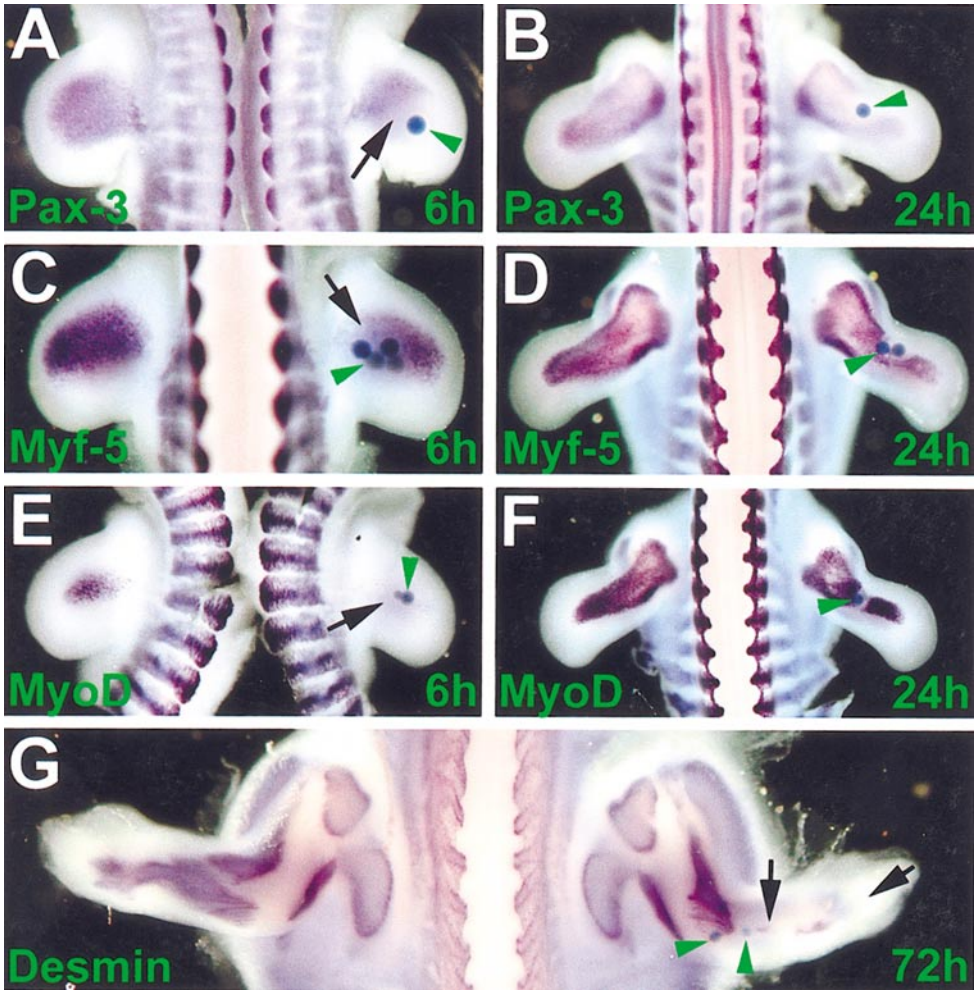

FIG. 7. Effect of ectopic myostatin on limb muscle development. Beads soaked in Myostatin (1 mg/ml) were implanted into the wing bud at stages 21–22. (A) Down-regulation of *Pax-3* expression (arrow) 6 h after Myostatin bead implantation in the right wing compared with the unoperated left wing. Bead (green arrowhead). (B) Twenty-four hours after Myostatin bead implantation, *Pax-3* expression is still down-regulated in the operated right wing compared with the unoperated left wing. Bead (green arrowhead). (C) Down-regulation of *Myf-5* expression (arrow) 6 h after Myostatin bead implantation in the right wing compared with the unoperated left wing. Beads (green arrowhead). (D) Twenty-four hours after Myostatin bead implantation, *Myf-5* expression is still down-regulated in the operated right wing compared with the unoperated left wing. Beads (green arrowhead). (E) Complete loss of *MyoD* expression (arrow) 6 h after Myostatin bead implantation in the right wing compared with the unoperated left wing. Bead (green arrowhead). (F) Twenty-four hours after Myostatin bead implantation, *MyoD* expression is still down-regulated in the operated right wing compared with the unoperated left wing. Bead (green arrowhead). (G) Exposure to Myostatin beads results in a lack of muscle especially in the zeugopod and autopod (arrows) in the operated right wing 72 h after operation compared with the unoperated left wing as revealed by Desmin expression. Beads (green arrowheads).

procedure, *Myostatin* expression is extended to the exposed surface. Thus, during limb development, *Myostatin* expression is found in nonproliferating mesenchymal cells. We previously have shown that the lack of proliferation signals emanated by the ectoderm results in muscle precursors to prematurely differentiate. However, sustained muscle development is inhibited, and we have proposed that this is due to the lack of precursors (which all precociously differentiated), which would be required for long-term growth (Amthor *et al.*, 1998). Sonic hedgehog, similar to the action of ectoderm, initially inhibits *MyoD* expression and transiently prevents muscle differentiation in the limb. Shh, probably via BMPs, induces the expression of *Pax-3* at the expense of *MyoD*. After a prolonged period of Pax-3-associated proliferation, more cells differentiate and muscle enlarges (Amthor *et al.*, 1998; Duprez *et al.*, 1998). Interestingly, Shh stimulates not only muscle growth, but enlarges the entire limb. Similarly, in this study, we show that

Myostatin expression is transiently down-regulated after exposure to Shh, but the *Myostatin* expression domain in the mesenchymal core eventually enlarges. This shows that signals such as ectoderm and Shh, which stimulate growth of limb tissues, inhibit expression of *Myostatin*.

We have shown that limb buds devoid of muscle still express *Myostatin*, albeit to a lesser extent than normal, which shows that nonmyogenic cells can express *Myostatin*. Centrally located mesenchymal cells normally develop into long bone rudiments (Mallein-Gerin *et al.*, 1988). However, Myostatin is unlikely to influence cartilage development as the femur in *Myostatin*$^{-/-}$ is relatively normal (Hamrick *et al.*, 2000). We suggest that, rather than acting on cartilage tissue, the centrally situated *Myostatin* expression acts to limit muscle growth of nearby premuscle masses. Thus, Myostatin acts in a similar fashion to Noggin, which is also expressed in the mesenchymal core of early limb buds and has been shown to inhibit muscle growth (Amthor *et al.*, 1998, 2002).

Remarkably, at late embryonic stages, *Myostatin* is up-regulated in a subset of limb bud muscles, and even within single muscles, *Myostatin* expression is not homogeneous. This expression pattern implies that Myostatin regulates differential growth of muscles. So far, it has not been reported whether size proportion between muscles is conserved in lack of Myostatin. Therefore, we currently can only speculate why the muscle size needs to be restricted during development. We suggest that, for optimal performance and reproductive fitness during normal life and under selective pressure, it is necessary to prevent overproduction of muscle while retaining the possibility to create more muscle in order to adapt to changing conditions. These changes could be simply brought about by modulating the expression of a single factor, such as Myostatin. It would be interesting to determine the survival fitness credentials under natural selection pressure in animals lacking Myostatin.

Application of Myostatin protein to developing limb buds results in a down-regulation of *Pax-3* and *Myf-5* expression, both genes which are associated with proliferation of myogenic precursors (Amthor *et al.*, 1998, Delfini *et al.*, 2000). Myostatin was also able to completely abolish the expression of *MyoD*, an early marker of muscle differentiation. Such inhibition of proliferation and differentiation of myogenic cells eventually results in a considerably decreased muscle mass production. Previous experiments suggested that limb muscle precursors either proliferate, differentiate, or are forced into apoptosis upon action of a wide range of growth factors, including Follistatin, Noggin, Shh, BMP-2, -4, and -7, and Delta (Delfini *et al.*, 2000; Amthor *et al.*, 1998, 2002; Hirsinger *et al.*, 1997; Pourquie *et al.*, 1996). Remarkably, myogenic cells, when exposed to Myostatin, loose gene expression of key transcription factors, which mark early muscle development. A possible explanation would be that myogenic cells are forced into programmed cell death; however, preliminary experiments fail to show this (data not published). Intriguingly, the effect of Myostatin appears to be stronger 6 h after treatment compared with 24 h after treatment. One possible explanation for these observations is that the effect of Myostatin to down-regulate *Pax-3*, *MyoD*, and *Myf5* is reversible. In this scenario, Myostatin would transiently delay muscle development, but once its potency had diminished, cells would be able to reenter the myogenic programme. Therefore, while the cells are not expressing *Pax-3*, the proliferating muscle precursor pool is not being expanded at its usual rate. Once the effect of ectopic Myostatin has worn off, the number of precursor cells that are able to rejoin the myogenic programme is considerably lower than that which would have normally developed. This suggestion implies that myogenic cells in the presence of Myostatin retain myogenic identity, albeit deprived of *Pax-3*, *Myf-5*, and *MyoD* expression. Another explanation for the loss of muscle is that myogenic cells loose their commitment towards the muscle lineage when exposed to Myostatin and adopt a differing fate. There is experimental precedent for this hypothesis from the elegant experiments of Tajbakhsh *et al.* (1996). They have demonstrated that, in lack of *Myf-5* (a gene that we have shown to be down-regulated by Myostatin), cells that would normally become muscle, develop into cartilage, bone, or dermal tissues. We currently investigate the fate of cells which have lost expression of myogenic marker genes after being exposed to Myostatin.

Myostatin and Head Development

In the head, expression of *Myostatin* only encompassed a small proportion of cells that develop into muscle. Expression of *Myostatin* appeared much later than expression of *Myf-5* and *MyoD* (Hacker and Guthrie, 1998). Furthermore, whereas *Myf-5* is expressed in branchial arches 1–3, expression of *Myostatin* was confined to branchial arches 1 and 2. However, even within these regions, its expression did not extend to the same proximal–distal extent as *Myf-5* expression, and, furthermore, expression was not confined to the core. The later observation is particularly interesting as it suggests that *Myostatin* expression may not be restricted to cells which originates from head mesenchyme, but that neural crest cells surrounding the core can also express the gene. This observation highlights the fact that, in myogenic regions, *Myostatin* can be expressed by both muscle and nonmuscle cells.

ACKNOWLEDGMENTS

We thank Professor Thomas Voit for his comments on the manuscript, and Ellen Gimbel for excellent technical assistance. This work was supported by a grant from the Deutsche Forschungsgemeinschaft (SFB 592, A1) (to B.C.); by a grant from the Wellcome Trust (to I.M.) (061425), by a grant from the Deutsche Forschungsgemeinschaft (Am 151/2-1), and from Hoffmann-La Roche (to H.A.).

REFERENCES

Amthor, H., Christ, B., and Patel, K. (1999). A molecular mechanism enabling continuous embryonic muscle growth: A balance between proliferation and differentiation. *Development* **126,** 1041–1053.

Amthor, H., Christ, B., Rashid-Doubell, F., Kemp, C. F., Lang, E., and Patel, K. (2002). Follistatin regulates bone morphogenetic protein-7 (BMP-7) activity to stimulate embryonic muscle growth. *Dev. Biol.* **243,** 115–127.

Amthor, H., Christ, B., Weil, M., and Patel, K. (1998). The importance of timing differentiation during limb muscle development. *Curr. Biol.* **8,** 642–652.

Amthor, H., Connolly, D., Patel, K., Brand-Saberi, B., Wilkinson, D. G., Cooke, J., and Christ, B. (1996). The expression and regulation of follistatin and a follistatin-like gene during avian somite compartmentalization and myogenesis. *Dev. Biol.* **178,** 343–362.

Bober, E., Brand-Saberi, B., Ebensperger, C., Wilting, J., Balling, R., Paterson, B. M., Arnold, H. H., and Christ, B. (1994). Initial steps of myogenesis in somites are independent of influence from axial structures. *Development* **120,** 3073–3082.

Chevallier, A., Kieny, M., and Mauger, A. (1977). Limb-somite relationship: Origin of the limb musculature. *J. Embryol. Exp. Morphol.* **41,** 245–258.

Christ, B., Amthor, H., Huang, R., Wagner, J., and Patel, K. (2001). Control of muscle mass development. In "The Origin and Fate of Somites" (E. J. Sanders, C. P. Lash, and C. P. Ordahl, Eds.). IOC Press, Amsterdam.

Christ, B., Brand-Saberi, B., Grim, M., and Wilting, J. (1992). Local signalling in dermomyotomal cell type specification. *Anat. Embryol. (Berl.)* **186,** 505–510.

Christ, B., Huang, R., and Wilting, J. (2000). The development of the avian vertebral column. *Anat. Embryol. (Berl.)* **202,** 179–194.

Christ, B., Jacob, H. J., and Jacob, M. (1974). Über den Ursprung der Flügelmuskulatur. Experimentelle Untersuchungen mit Wachtel- und Hühnerembryonen. *Experientia* **30,** 1446–1449.

Christ, B., Jacob, H. J., and Jacob, M. (1977). Experimental analysis of the origin of the wing musculature in avian embryos. *Anat. Embryol. (Berl.)* **150,** 171–186.

Christ, B., and Ordahl, C. P. (1995). Early stages of chick somite development. *Anat. Embryol. (Berl.)* **191,** 381–396.

Cinnamon, Y., Kahane, N., and Kalcheim, C. (1999). Characterization of the early development of specific hypaxial muscles from the ventrolateral myotome. *Development* **126,** 4305–4315.

Cohn, M. J., Izpisua-Belmonte, J. C., Abud, H., Heath, J. K., and Tickle, C. (1995). Fibroblast growth factors induce additional limb development from the flank of chick embryos. *Cell* **80,** 739–746.

Delfini, M., Hirsinger, E., Pourquie, O., and Duprez, D. (2000). Delta 1-activated notch inhibits muscle differentiation without affecting Myf5 and Pax3 expression in chick limb myogenesis. *Development* **127,** 5213–5224.

Denetclaw, W. F., Jr., Berdougo, E., Venters, S. J., and Ordahl, C. P. (2001). Morphogenetic cell movements in the middle region of the dermomyotome dorsomedial lip associated with patterning and growth of the primary epaxial myotome. *Development* **128,** 1745–1755.

Denetclaw, W. F., Jr., Christ, B., and Ordahl, C. P. (1997). Location and growth of epaxial myotome precursor cells. *Development* **124,** 1601–1610.

Denetclaw, W. F., and Ordahl, C. P. (2000). The growth of the dermomyotome and formation of early myotome lineages in thoracolumbar somites of chicken embryos. *Development* **127,** 893–905.

Duprez, D., Fournier-Thibault, C., and Le Douarin, N. (1998). Sonic Hedgehog induces proliferation of committed skeletal muscle cells in the chick limb. *Development* **125,** 495–505.

Franz, T., Kothary, R., Surani, M. A., Halata, Z., and Grim, M. (1993). The Splotch mutation interferes with muscle development in the limbs. *Anat. Embryol. (Berl.)* **187,** 153–160.

Gonzalez-Cadavid, N. F., Taylor, W. E., Yarasheski, K., Sinha-Hikim, I., Ma, K., Ezzat, S., Shen, R., Lalani, R., Asa, S., Mamita, M., Nair, G., Arver, S., and Bhasin, S. (1998). Organization of the human myostatin gene and expression in healthy men and HIV-infected men with muscle wasting. *Proc. Natl. Acad. Sci. USA* **95,** 14938–14943.

Hacker, A., and Guthrie, S. (1998). A distinct developmental programme for the cranial paraxial mesoderm in the chick embryo. *Development* **125,** 3461–3472.

Hamburger, V., and Hamilton, H. L. (1992). A series of normal stages in the development of the chick embryo. 1951. *Dev. Dyn.* **195,** 231–272.

Hamrick, M. W., McPherron, A. C., Lovejoy, C. O., and Hudson, J. (2000). Femoral morphology and cross-sectional geometry of adult myostatin-deficient mice. *Bone* **27,** 343–349.

Hirsinger, E., Duprez, D., Jouve, C., Malapert, P., Cooke, J., and Pourquie, O. (1997). Noggin acts downstream of Wnt and Sonic Hedgehog to antagonize BMP4 in avian somite patterning. *Development* **124,** 4605–4614.

Hirsinger, E., Malapert, P., Dubrulle, J., Delfini, M. C., Duprez, D., Henrique, D., Ish-Horowicz, D., and Pourquie, O. (2001). Notch signalling acts in postmitotic avian myogenic cells to control MyoD activation. *Development* **128,** 107–116.

Huang, R., and Christ, B. (2000). Origin of the epaxial and hypaxial myotome in avian embryos. *Anat. Embryol. (Berl.)* **202,** 369–374.

Huang, R., Zhi, Q., Izpisua-Belmonte, J. C., Christ, B., and Patel, K. (1999). Origin and development of the avian tongue muscles [In Process Citation]. *Anat. Embryol. (Berl.)* **200,** 137–152.

Ji, S., Losinski, R. L., Cornelius, S. G., Frank, G. R., Willis, G. M., Gerrard, D. E., Depreux, F. F., and Spurlock, M. E. (1998). Myostatin expression in porcine tissues: tissue specificity and developmental and postnatal regulation. *Am. J. Physiol.* **275,** R1265–R1273.

Kahane, N., Cinnamon, Y., Bachelet, I., and Kalcheim, C. (2001). The third wave of myotome colonization by mitotically competent progenitors: Regulating the balance between differentiation and proliferation during muscle development. *Development* **128,** 2187–2198.

Kahane, N., Cinnamon, Y., and Kalcheim, C. (1998). The cellular mechanism by which the dermomyotome contributes to the second wave of myotome development. *Development* **125,** 4259–4271.

Kambadur, R., Sharma, M., Smith, T. P., and Bass, J. J. (1997). Mutations in myostatin (GDF8) in double-muscled Belgian Blue and Piedmontese cattle. *Genome Res.* **7,** 910–916.

Kirk, S., Oldham, J., Kambadur, R., Sharma, M., Dobbie, P., and Bass, J. (2000). Myostatin regulation during skeletal muscle regeneration. *J. Cell Physiol.* **184,** 356–363.

Kocamis, H., Kirkpatrick-Keller, D. C., Richter, J., and Killefer, J. (1999). The ontogeny of myostatin, follistatin and activin-B

mRNA expression during chicken embryonic development. *Growth Dev. Aging* **63,** 143–150.

Le Lievre, C. S., and Le Douarin, N. M. (1975). Mesenchymal derivatives of the neural crest: Analysis of chimaeric quail and chick embryos. *J. Embryol. Exp. Morphol.* **34,** 125–154.

Lee, S. J., and McPherron, A. C. (1999). Myostatin and the control of skeletal muscle mass. *Curr. Opin. Genet. Dev.* **9,** 604–607.

Li, L., Cserjesi, P., and Olson, E. N. (1995). Dermo-1: A novel twist-related bHLH protein expressed in the developing dermis. *Dev. Biol.* **172,** 280–292.

Mallein-Gerin, F., Kosher, R. A., Upholt, W. B., and Tanzer, M. L. (1988). Temporal and spatial analysis of cartilage proteoglycan core protein gene expression during limb development by in situ hybridization. *Dev. Biol.* **126,** 337–345.

Marti, E., Takada, R., Bumcrot, D. A., Sasaki, H., and McMahon, A. P. (1995). Distribution of Sonic hedgehog peptides in the developing chick and mouse embryo. *Development* **121,** 2537–2547.

McPherron, A. C., Lawler, A. M., and Lee, S. J. (1997). Regulation of skeletal muscle mass in mice by a new TGF-beta superfamily member. *Nature* **387,** 83–90.

McPherron, A. C., and Lee, S. J. (1997). Double muscling in cattle due to mutations in the myostatin gene. *Proc. Natl. Acad. Sci. USA* **94,** 12457–12461.

Miller, J. B., and Stockdale, F. E. (1986). Developmental regulation of the multiple myogenic cell lineages of the avian embryo. *J. Cell Biol.* **103,** 2197–2208.

Mootoosamy, R. C., and Dietrich, S. (2002). Distinct regulatory cascades for head and trunk myogenesis. *Development* **129,** 573–583.

Nieto, M. A., Patel, K., and Wilkinson, D. G. (1996). In situ hybridization analysis of chick embryos in whole mount and tissue sections. *Methods Cell Biol.* **51,** 219–235.

Olivera-Martinez, I., Coltey, M., Dhouailly, D., and Pourquie, O. (2000). Mediolateral somitic origin of ribs and dermis determined by quail-chick chimeras. *Development* **127,** 4611–4617.

Ordahl, C. P., Berdougo, E., Venters, S. J., and Denetclaw, W. F., Jr. (2001). The dermomyotome dorsomedial lip drives growth and morphogenesis of both the primary myotome and dermomyotome epithelium. *Development* **128,** 1731–1744.

Pourquie, O., Fan, C. M., Coltey, M., Hirsinger, E., Watanabe, Y., Breant, C., Francis-West, P., Brickell, P., Tessier-Lavigne, M., and Le Douarin, N. M. (1996). Lateral and axial signals involved in avian somite patterning: a role for BMP4. *Cell* **84,** 461–471.

Pownall, M. E., and Emerson, C. P., Jr. (1992). Sequential activation of three myogenic regulatory genes during somite morphogenesis in quail embryos. *Dev. Biol.* **151,** 67–79.

Rong, P. M., Teillet, M. A., Ziller, C., and Le Douarin, N. M. (1992). The neural tube/notochord complex is necessary for vertebral but not limb and body wall striated muscle differentiation. *Development* **115,** 657–672.

Sakuma, K., Watanabe, K., Sano, M., Uramoto, I., and Totsuka, T. (2000). Differential adaptation of growth and differentiation factor 8/myostatin, fibroblast growth factor 6 and leukemia inhibitory factor in overloaded, regenerating and denervated rat muscles. *Biochim. Biophys. Acta* **1497,** 77–88.

Schmidt, M., Tanaka, M., and Munsterberg, A. (2000). Expression of β-catenin in the developing chick myotome is regulated by myogenic signals [In Process Citation]. *Development* **127,** 4105–4113.

Sharma, M., Kambadur, R., Matthews, K. G., Somers, W. G., Devlin, G. P., Conaglen, J. V., Fowke, P. J., and Bass, J. J. (1999). Myostatin, a transforming growth factor-beta superfamily member, is expressed in heart muscle and is upregulated in cardiomyocytes after infarct. *J. Cell Physiol.* **180,** 1–9.

Solursh, M., and Reiter, R. S. (1988). Inhibitory and stimulatory effects of limb ectoderm on in vitro chondrogenesis. *J. Exp. Zool.* **248,** 147–154.

Stockdale, F. E. (1992). Myogenic cell lineages. *Dev. Biol.* **154,** 284–298.

Tajbakhsh, S., Rocancourt, D., and Buckingham, M. (1996). Muscle progenitor cells failing to respond to positional cues adopt non-myogenic fates in myf-5 null mice. *Nature* **384,** 266–270.

Tajbakhsh, S., Rocancourt, D., Cossu, G., and Buckingham, M. (1997). Redefining the genetic hierarchies controlling skeletal myogenesis: Pax-3 and Myf-5 act upstream of MyoD. *Cell* **89,** 127–138.

Taylor, W. E., Bhasin, S., Artaza, J., Byhower, F., Azam, M., Willard, D. H., Kull, F. C., and Gonzalez-Cadavid, N. (2001). Myostatin inhibits cell proliferation and protein synthesis in C(2)C(12) muscle cells. *Am. J. Physiol. Endocrinol. Metab.* **280,** E221–E228.

Thomas, M., Langley, B., Berry, C., Sharma, M., Kirk, S., Bass, J., and Kambadur, R. (2000). Myostatin, a negative regulator of muscle growth, functions by inhibiting myoblast proliferation. *J. Biol. Chem.* **275,** 40235–40243.

Wachtler, F., and Jacob, M. (1986). Origin and development of the cranial skeletal muscles. *Bibl. Anat.* **29,** 24–46.

Zhu, X., Hadhazy, M., Wehling, M., Tidball, J. G., and McNally, E. M. (2000). Dominant negative myostatin produces hypertrophy without hyperplasia in muscle. *FEBS Lett.* **474,** 71–75.

Received for publication February 14, 2002
Revised June 7, 2002
Accepted July 10, 2002
Published online October 10, 2002